Measurement of $t\bar{t}$ normalised multi-differential cross sections in pp collisions at $\sqrt{s} = 13$ TeV, and simultaneous determination of the strong coupling strength, top quark pole mass, and parton distribution functions

arXiv:1904.05237v1

JC105

05/05/2019

1a. Introduction： generation of ttbar

$$\sigma_{t\bar{t}+X} = \int_0^1 dx_1 \int_0^1 dx_2 \sum_{ij} f_i(x_1, \mu_F) f_j(x_2, \mu_F) \hat{\sigma}_{ij \to t\bar{t}+X}(\sqrt{\hat{s}})$$

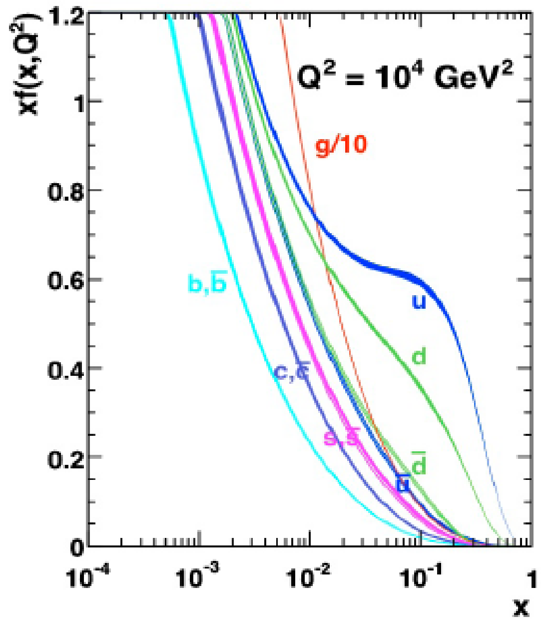

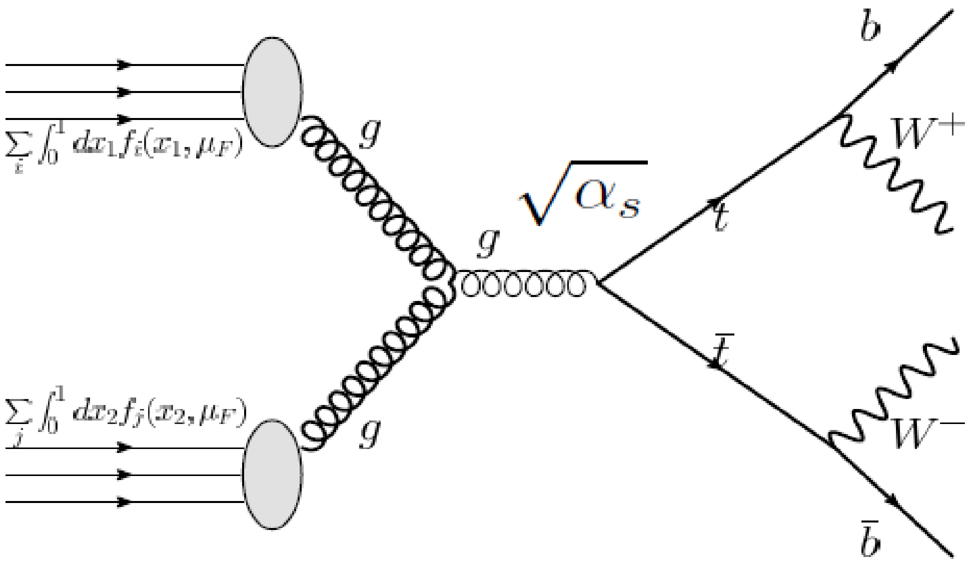

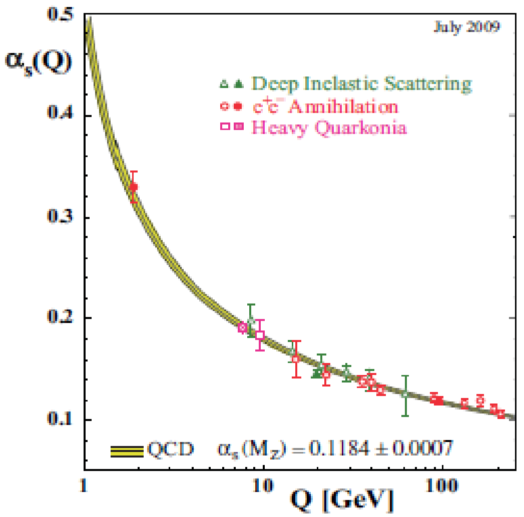

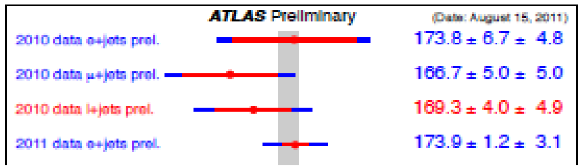

- ttbar is mainly generated via gluon fusion at p-p collider
- cross section depends on PDF (of partons inside proton) , coupling , mass and so on.

1b. Introduction： top mass

・ Since its decay width is wider than that of QCD, top quark decays W+b quark before hadronization :

$$\Gamma_t \simeq \frac{G_F m_t^3}{8\sqrt{2}\pi}|V_{tb}| \sim 1.5\ \mathrm{GeV} \gg \Lambda_{QCD}(\sim 300\ \mathrm{MeV})$$

Then, calculating the invariant mass from all of decay products, the mass of top quark can be deduced . . .

This is just robust estimation, since the initial top quark has color, whereas the decay products are all color singlet.

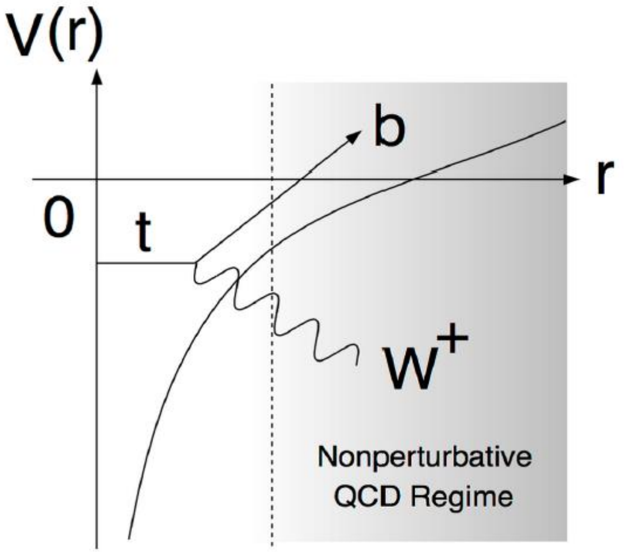

1c. Introduction： top mass

Question from Xin： Could you explain a bit more on "top quark pole mass"?

A. Pole mass is defined as the pole position of the propagator

$$S_F(\not{p})^{-1} = \not{p} - m - \Sigma(\not{p}) \simeq \not{p} - m_{pole}$$

-- Somehow close to the value obtained from the cross section

-- But, quark does not freely moving like electrons, , ,

-- Need to calculate the correction factor which is not trivial as leptons, owing to its strong coupling, α_s (. . . definitely need to calculate higher order because of bad covergence)

i.e.) propagator for electron at Dirac field is

$$\tilde{S}_F(p) = \frac{1}{\gamma^\mu p_\mu - m + i\epsilon} = \frac{1}{\not{p} - m + i\epsilon}.$$

Precise determination of top quark mass is one of hot topic

2. The Compact Muon Solenoid (CMS) detector

From
https://cms.cern/detector

・ at 15 metres high and 21 metres long, it really is quite **compact** for all the detector material it containts;

・ it is designed to detect particles known as **muons** very accurately; and

・ it has the most powerful **solenoid** magnet ever made.

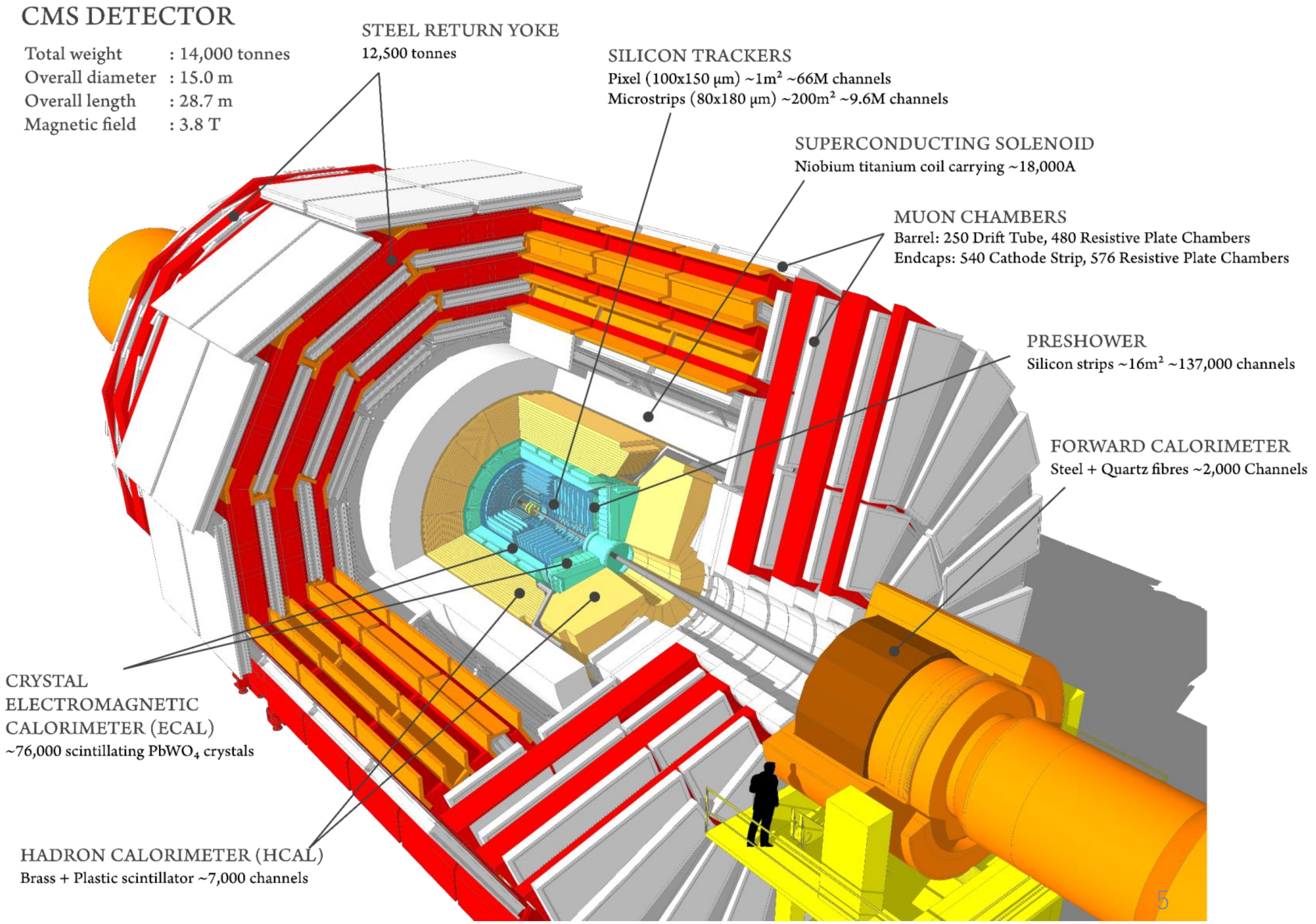

3a. Event Selection

- Signal :
  leptons (e^+e^-, $\mu^+\mu^-$, or $e^\pm\mu^\mp$)
  from W bosons +
  two jets (=b quark)

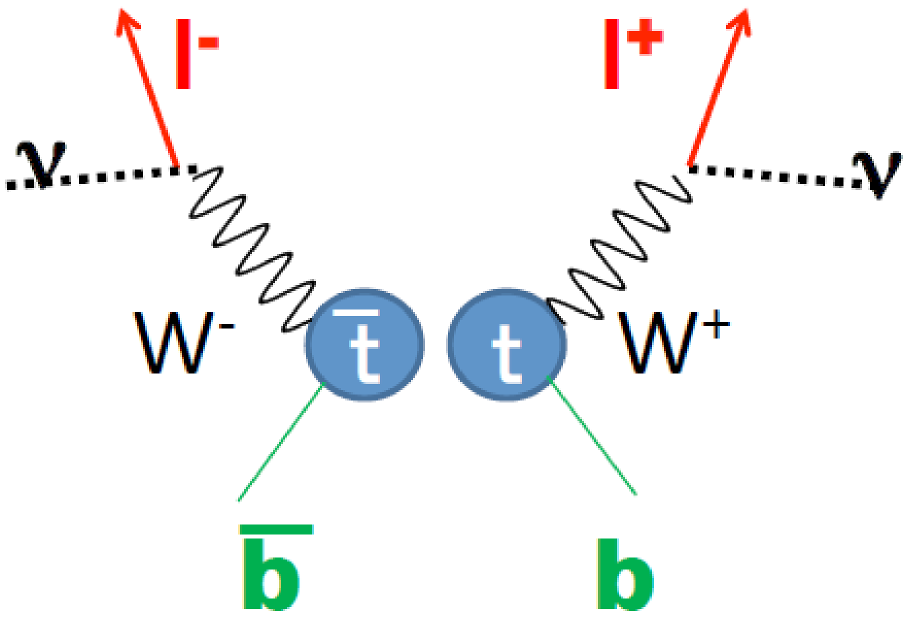

- Reconstruction :
  -- P_T cut (for leptons)
  -- Using a particle-flow algorithm
  -- Jets , clustering the PF candidates using anti-k_T algorithm with R=0.4
  -- Ranking the combinations (for multi-candidates)
  -- ....

Ref : Backgrounds （taken from an ATLAS analysis slide ）

Backgrounds due to detector effects

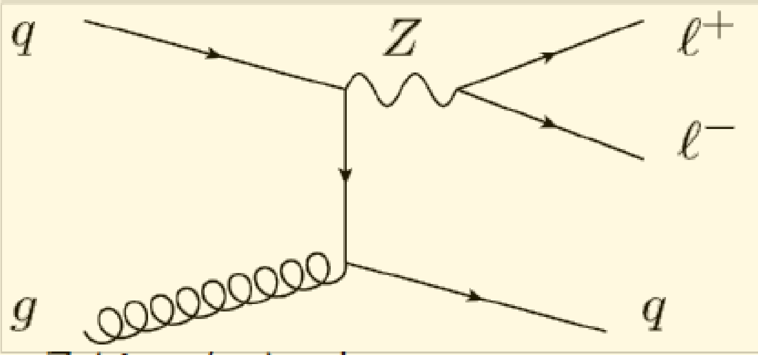

Z (→ee/μμ) + jets (1.0×10³pb)

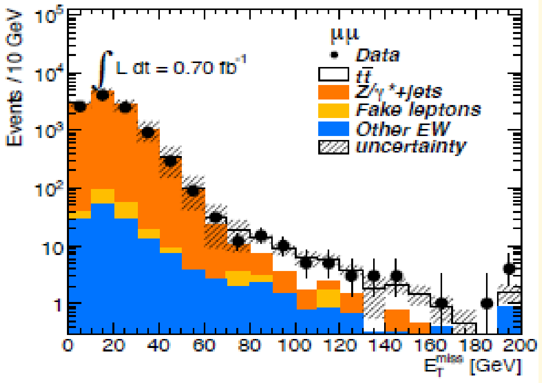

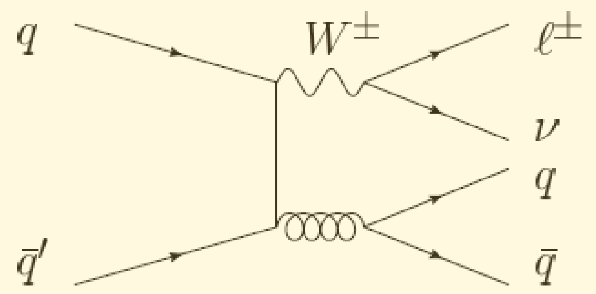

W (→eν/μν) + jets (10⁴pb)

Backgrounds that have similar event topologies (two leptons, neutrino)

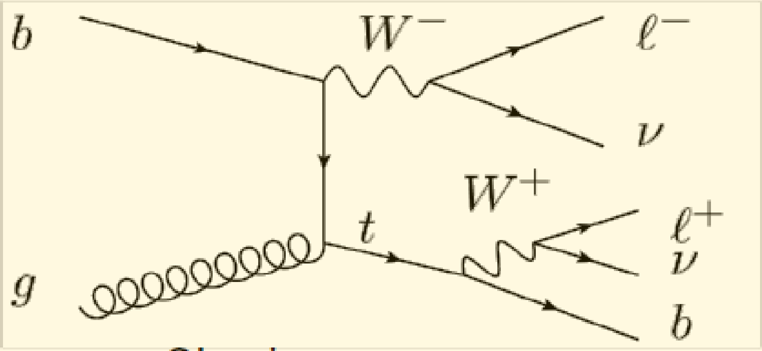

Single top (1.0pb)

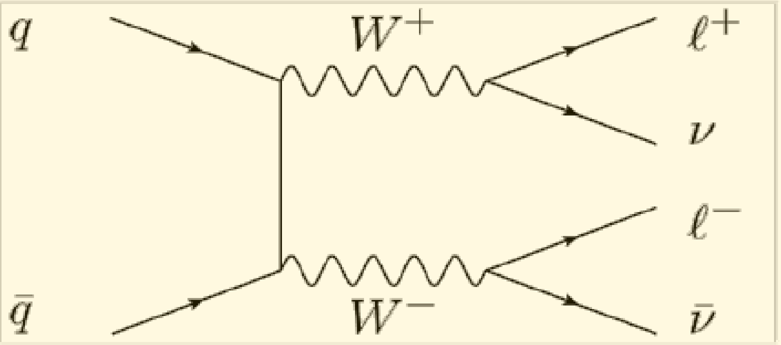

Diboson (7.6pb)

3b. Event Selection

From Figure 1.

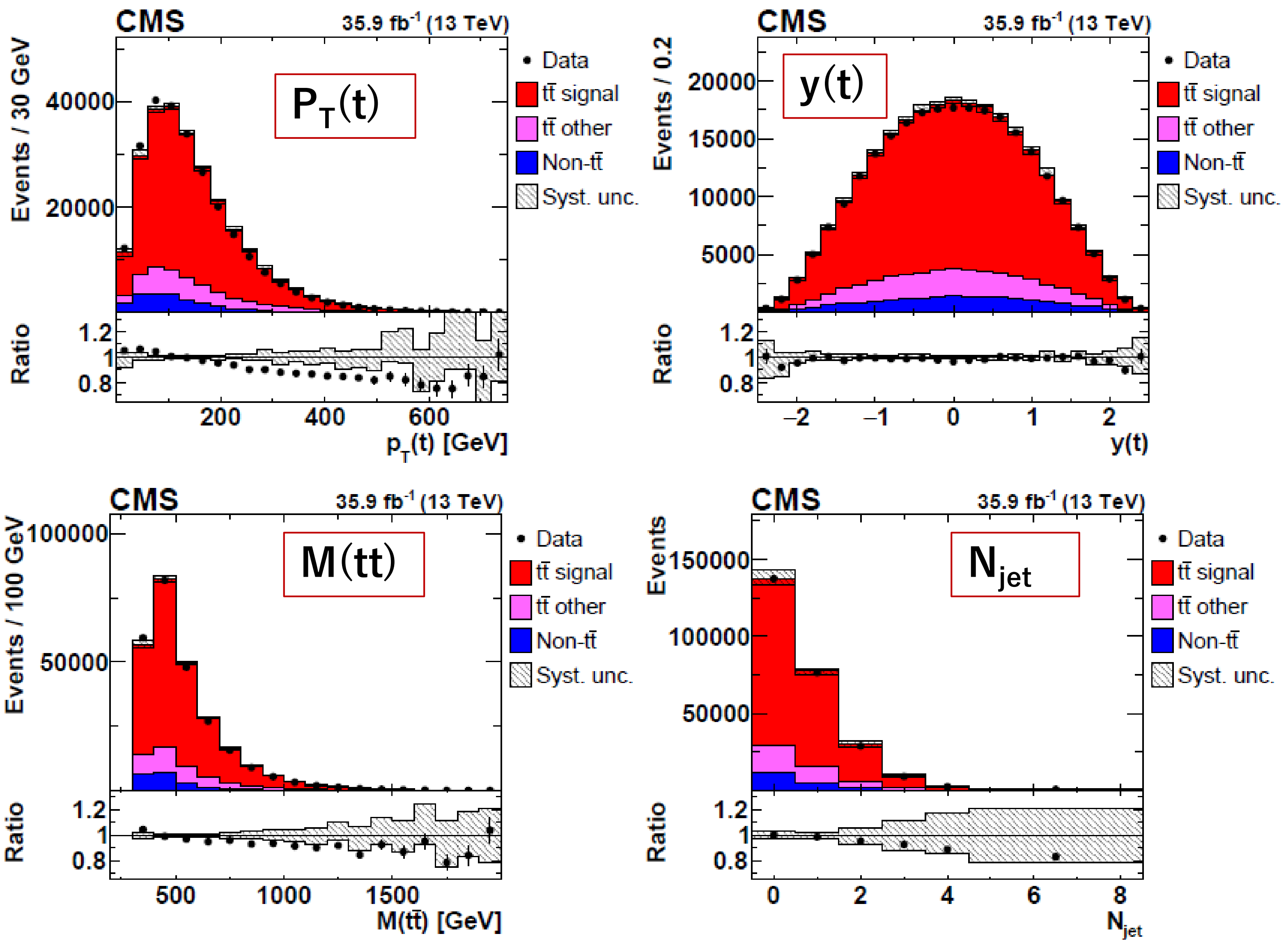

y(t) : rapidity of the top quark

N_{jet} : number of extra jets not arising from the decay of the tt system

4. Unfolding and cross section

・ Background subtraction , where the number of background events are obtained directly from MC simulations.

・ Only W->τ->l(e or μ) background channel are almost identical to the signal, thus it is normalized.

・ The number of signal events after background subtraction are corrected for detector effects

Here, “response matrix” is used for this unfolding procedure, which returns the full phase space for tt production at parton level .

・ Cross section :

$$\frac{\sigma_i}{\sigma} = \frac{1}{\sigma} \frac{\hat{M}_i^{\mathrm{unf}}}{\mathcal{B}\,\mathcal{L}}$$

where M_i^{unf} is the number of unfolded signal events in bins ***i*** **,**
B is the branching ratio of tt into the lepton final states **.**

5a. Results: double-differential cross section

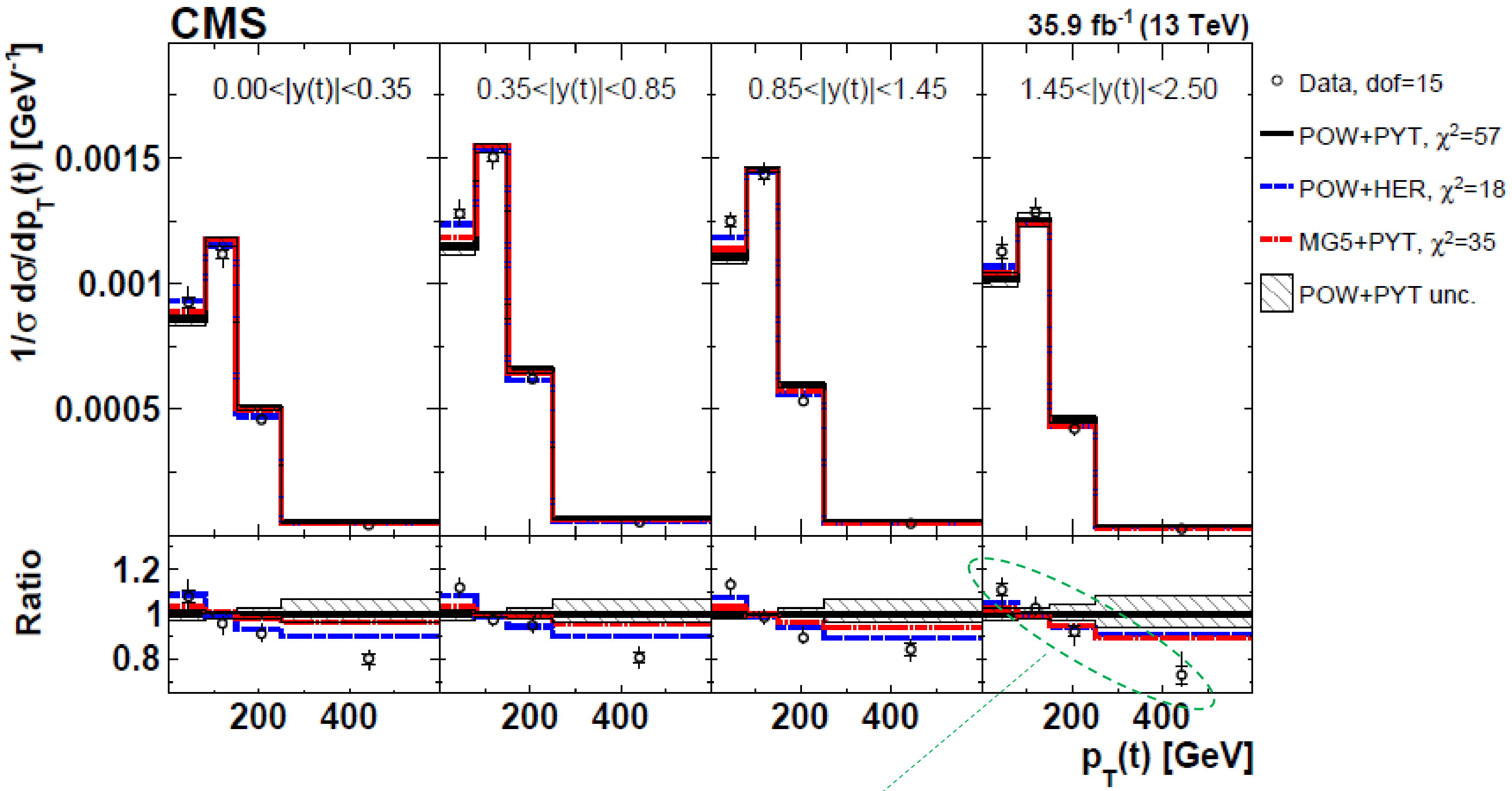

Figure 3: Comparison of the measured $[y(t), p_T(t)]$ cross sections to the theoretical predictions

From the paper, "The data distribution is softer than that of the predictions . . . "

5b. Results: triple-differential cross section

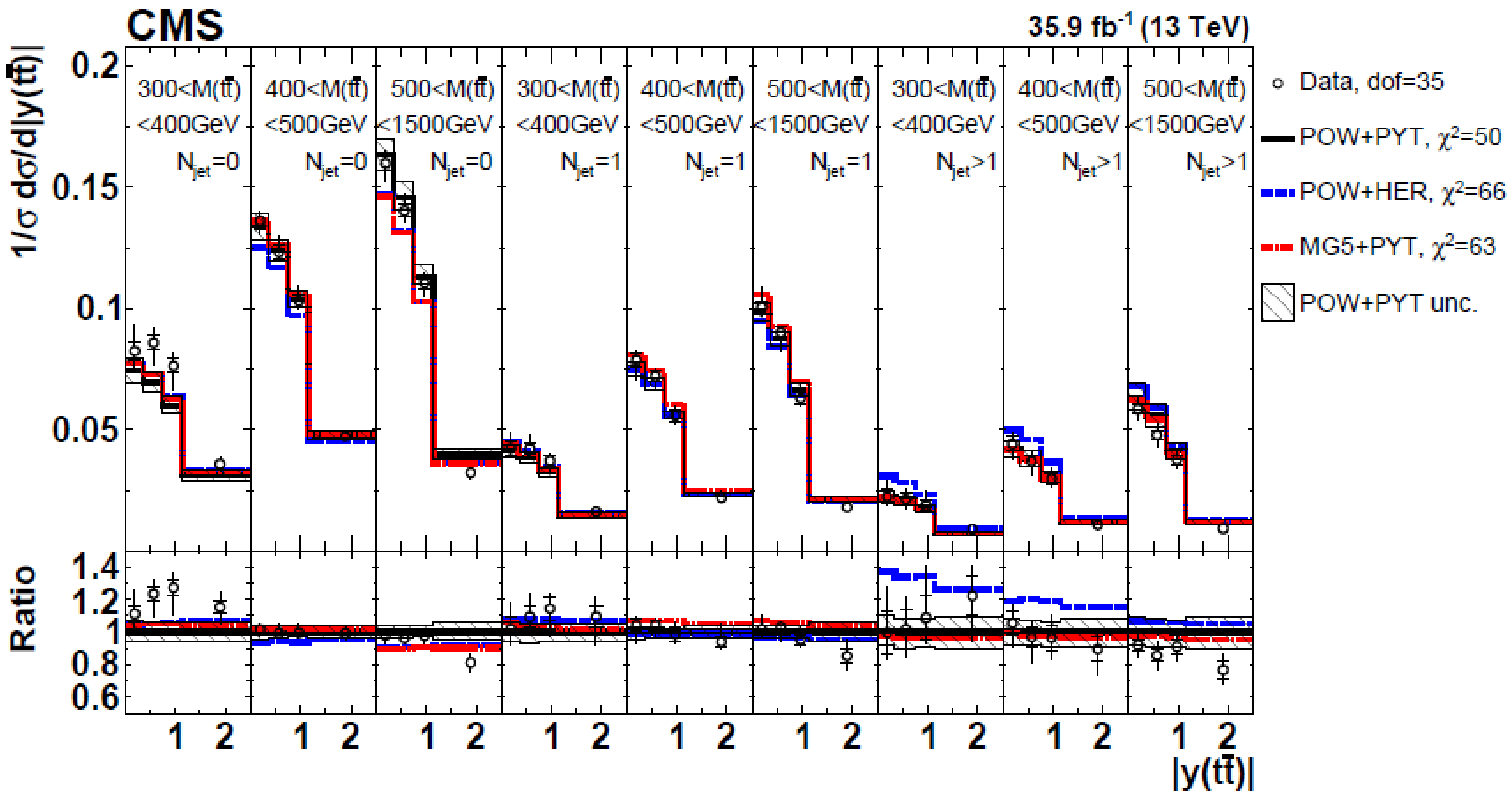

Figure 11: Comparison of the measured $[N_{\mathrm{jet}}^{0,1,2+}, M(\mathrm{t\bar{t}}), y(\mathrm{t\bar{t}})]$ cross sections to the theoretical predictions calculated using MC event generators (further details can be found in the Fig. 3 caption).

From the paper, “POW+HER predicts too high a cross section for $N_{\mathrm{jet}}>1$ . . . ”

6a. Extraction of α_s and m_t^{pole} using external PDFs

To extract α_s and m_t^{pole}, the measured triple-differential cross sections are compared to fixed-order NLO predictions

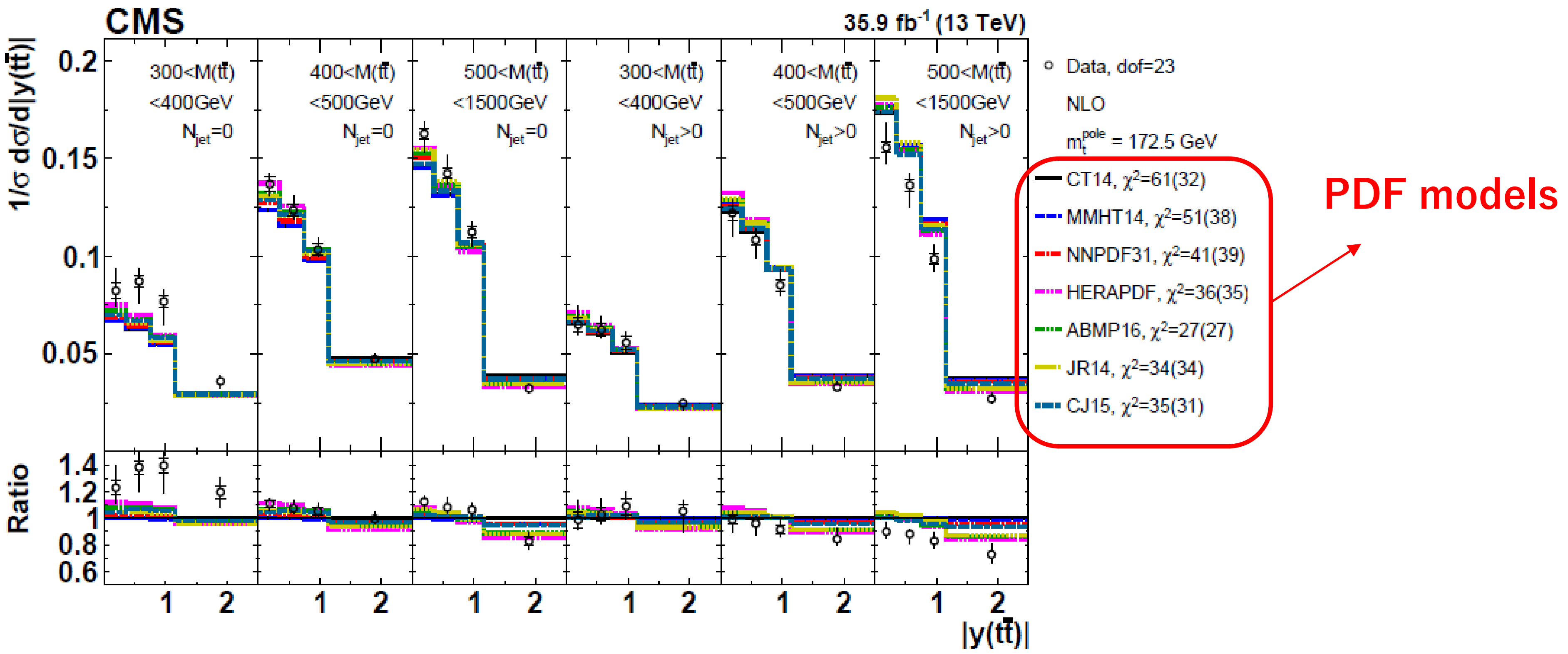

Figure 14: Comparison of the measured $[N_{\mathrm{jet}}^{0,1+}, M(\mathrm{t\bar{t}}), y(\mathrm{t\bar{t}})]$ cross sections to NLO predictions obtained using different PDF sets (further details can be found in Fig. 3). For each theoretical

6b. Extraction of α_s and m_t^{pole} using external PDFs

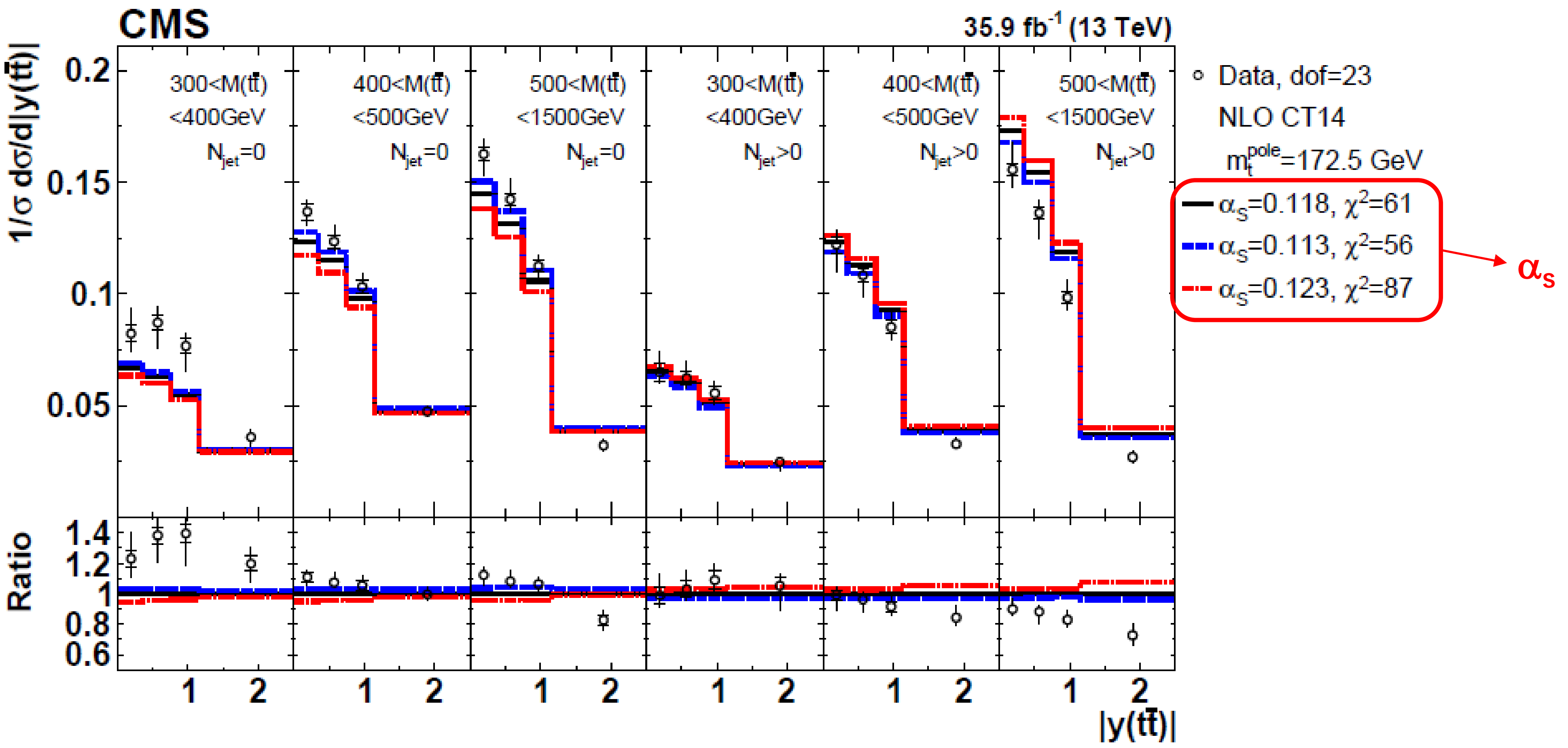

Figure 15: Comparison of the measured [$N_{\text{jet}}^{0,1+}$, $M(\text{t}\bar{\text{t}})$, $y(\text{t}\bar{\text{t}})$] cross sections to NLO predictions obtained using different $\alpha_S(m_Z)$ values (further details can be found in Fig. 3). For each

6c. Extraction of α_s and m_t^{pole} using external PDFs

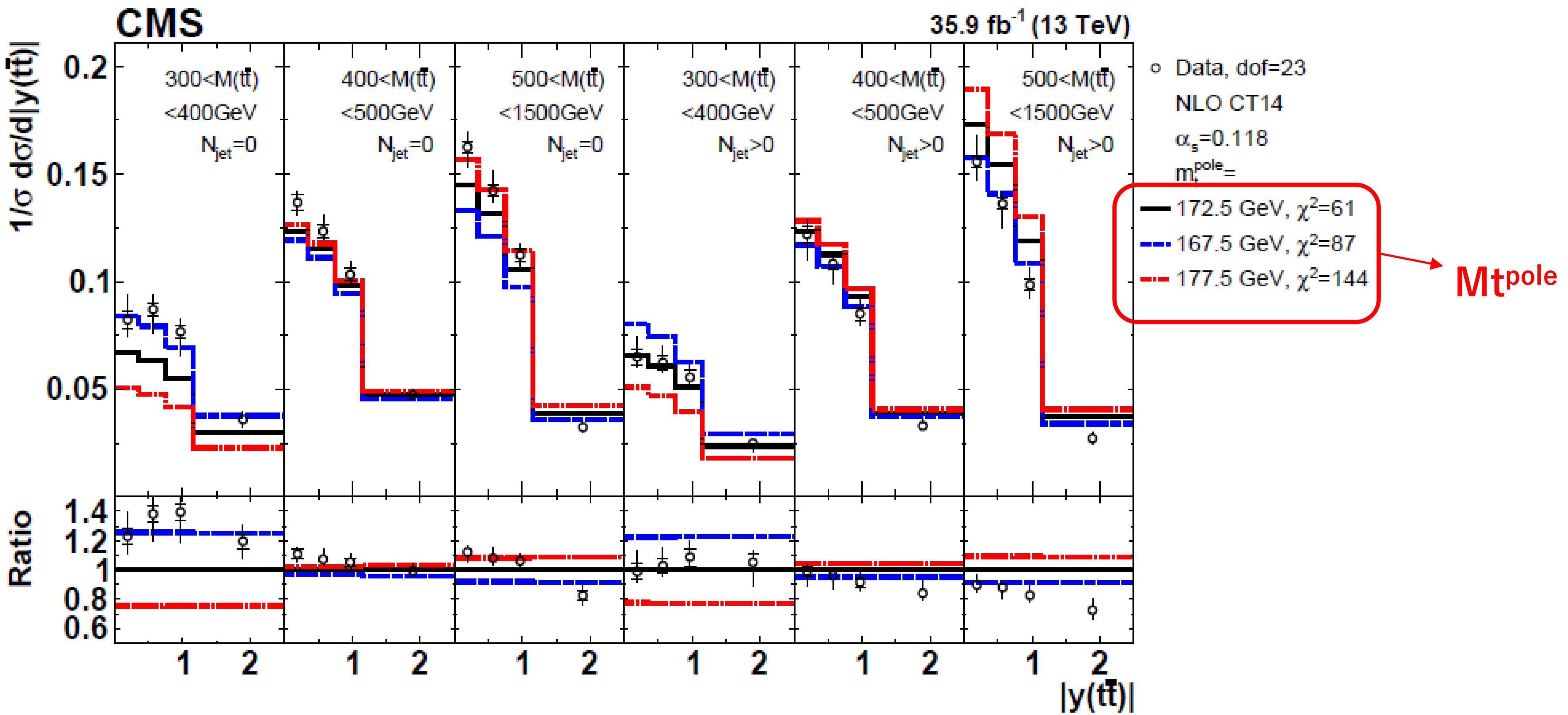

Figure 16: Comparison of the measured $[N_{\mathrm{jet}}^{0,1+}, M(\mathrm{t\bar{t}}), y(\mathrm{t\bar{t}})]$ cross sections to NLO predictions obtained using different m_t^{pole} values (further details can be found in Fig. 3). For each theoretical

Really, model dependent ….

6d. Simultaneous PDF, α_s and m_t^{pole} fit

The measured triple-differential cross sections are used in a simultaneous PDF, α_s and m_t^{pole} fit at NLO, together with the combined HERA inclusive deep inelastic scattering data.

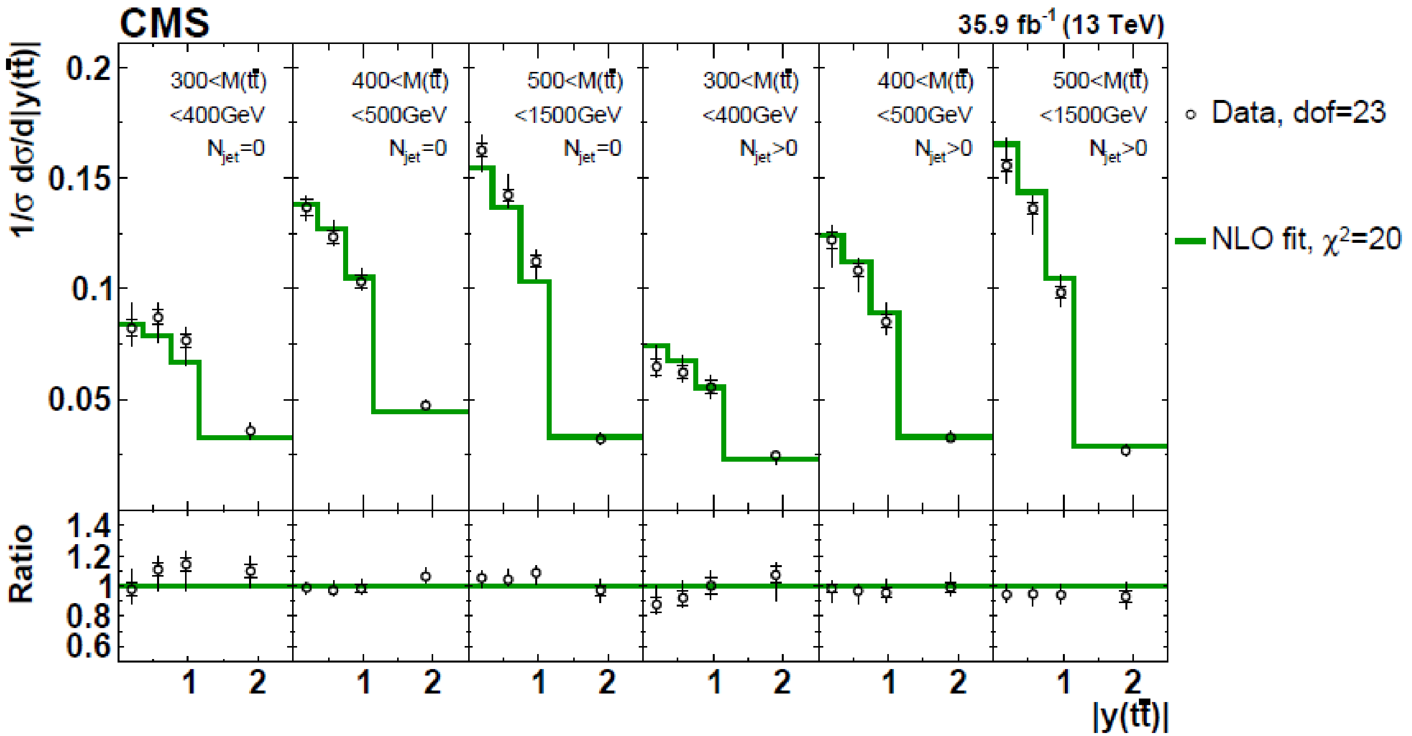

Figure 19: Comparison of the measured $[N_{jet}^{0,1+}, M(t\bar{t}), y(t\bar{t})]$ cross sections to the NLO predictions using the parameter values from the simultaneous PDF, α_S, and m_t^{pole} fit (further details

7. Summary

A measurement was presented of normalised multi-differential $t\bar{t}$ production cross sections in pp collisions at $\sqrt{s} = 13\,\text{TeV}$, performed using events containing two oppositely charged leptons (electron or muon). The analysed data were recorded in 2016 with the CMS detector at the LHC, and correspond to an integrated luminosity of $35.9\,\text{fb}^{-1}$. The normalised $t\bar{t}$ cross section is measured in the full phase space as a function of different pairs of kinematic variables that describe either the top quark or the $t\bar{t}$ system. None of the central predictions of the tested Monte Carlo models is able to correctly describe all the distributions. The data exhibit softer transverse momentum $p_T(t)$ distributions than given by the theoretical predictions, as was reported in previous single-differential and double-differential $t\bar{t}$ cross section measurements. The effect of the softer $p_T(t)$ spectra in the data relative to the predictions is enhanced at larger values of the invariant mass of the $t\bar{t}$ system. The predicted $p_T(t)$ slopes are strongly sensitive to the parton distribution functions (PDFs) and the top quark pole mass m_t^{pole} value used in the calculations, and the description of the data can be improved by changing these parameters.